

Ultrafast switching of magnetic nanoelements using a rotating field

J. Fidler, T. Schrefl, V. D. Tsiantos, W. Scholz, D. Suess, and H. Forster
Vienna University of Technology Wiedner Hauptstr. 8, A-1040 Vienna, Austria

Nanostructured granular $\text{Ni}_{80}\text{Fe}_{20}$ and Co films are studied using a 3D hybrid finite element/boundary element model. Switching dynamics are calculated for external fields applied unidirectional after a rise time of 0.1 ns and for a 10 GHz rotational field with a field strength of $H_{\text{ext}} = 0.2 J_s / \mu_0$ (160 kA/m for NiFe and 280 kA/m for Co). The transient magnetization patterns show that reversal in the unidirectional field proceeds by the nucleation and propagation of end domains towards the center of the element. The switching time strongly depends on the Gilbert damping parameter α . Materials with uniaxial anisotropy (Co), require larger field, but exhibit shorter switching times. Reversal in rotational fields involves inhomogeneous rotation of the end domains towards the rotational field direction leading to partial flux-closure structures. Shorter switching times are obtained by the application of the 10 GHz rotational field ($t_{\text{sw}} = 0.05$ ns). Precessional oscillation effects after abruptly switching off the external field which occurred in the NiFe square element, were suppressed in the granular Co film. Reducing the field to zero slowly inhibits the high frequency excitations in NiFe. © 2002 American Institute of Physics. [DOI: 10.1063/1.1452648]

I. INTRODUCTION

The numerical solution of the Landau–Lifshitz–Gilbert equation of motion provides the theoretical background for the switching process of ferromagnetic structures. Kikuchi¹ derived the difference of the minimum reversal times in a sphere and a magnetic thin film depending on the damping parameter. In small hard magnetic particles a waiting time after the application of an applied field, before the nucleation of reversed domains is initiated, has been observed.^{2–4} With decreasing size of the magnetic structures, thermally activated reversal process become significant. Thermally induced reversal may influence the writing process as well as the long-term stability of written bits in magnetic recording. Zhang and Fredkin^{5,6} used the finite element method to study thermally activated reversal in ellipsoidal particles large enough to show an inhomogeneous reversal process. We present a three dimensional (3D) micromagnetic simulation using a hybrid finite element/boundary element model and taking into account realistic magnetic field profiles with time to investigate the switching behavior of permalloy with zero anisotropy and uniaxial granular Co nanoelements. The influence of a rotational field with variable field strength and rotation speed is compared with an unidirectional field with variable field rise and decay times. Thermal fluctuations, defects and other forms of disorder as well as eddy-currents occurring during the fast switching process are not included.

II. MICROMAGNETIC SIMULATION MODEL

We have used a 3D numerical micromagnetic model with tetrahedral finite elements⁷ with a constant edge length between 2.5 nm and 5 nm to study a thin nanostructured square of $\text{Ni}_{80}\text{Fe}_{20}$ with dimensions of $100 \times 100 \times 20 \text{ nm}^3$ and a polycrystalline Co square shaped element consisting of 100 randomly oriented grains with uniaxial magnetocrystalline anisotropy and an average diameter of about 10 nm with dimensions of $100 \times 100 \times 10 \text{ nm}^3$. Generally, the numerical

results are independent of the mesh size, if the finite element size is smaller than the exchange length, which is determined by the Néel or Bloch wall parameters. The time evolution of the magnetization at each nodal point of the finite element mesh was calculated using the Gilbert equation of motion, which describes the physical path of the magnetic polarization \mathbf{J} toward equilibrium:

$$\frac{d\mathbf{J}}{dt} = -|\gamma_0| \mathbf{J} \times \mathbf{H}_{\text{eff}} + \frac{\alpha}{J_s} \mathbf{J} \times \frac{\partial \mathbf{J}}{\partial t}. \quad (1)$$

At each time step, which is in the order of fs, the effective field term H_{eff} include the applied field, the exchange field, the magneto-crystalline anisotropy field and the demagnetizing field. The term γ_0 is the gyromagnetic ratio of the free electron spin and α is the damping constant. The first term on the right hand side of Eq. (1) accounts for the gyromagnetic precession of the magnetic polarization \mathbf{J} , the second term arises from viscous damping. At high damping the magnetization rotates more or less directly toward the field direction, as the second term is dominant. In order to apply various profiles for the external field or study the effect a rotating external field, the strength and direction of the external field is treated as a continuous function of time

$$\mathbf{H}_{\text{ext}} = \mathbf{H}_{\text{ext}}(t) = H(t) \cdot [\cos(\phi(t)) \cdot \sin(\theta(t)), \sin(\phi(t)) \cdot \sin(\theta(t)), \cos(\theta(t))] \quad (2)$$

during the time integration of the Landau–Lifshitz–Gilbert equation. In Eq. (2) ϕ and θ are the angle of the external field with respect to the x - and z -axis of a Cartesian coordinate system. For a rotating field in the (x,y) plane θ equals $\pi/2$ and (2) writes

$$\mathbf{H}_{\text{ext}}(t) = H \cdot [\cos(\omega \cdot t), \sin(\omega \cdot t), 0], \quad (3)$$

where $\omega = 2\pi/T$ is the angular frequency. We use an implicit time integration scheme⁸ to solve the Landau–Lifshitz–Gilbert equation. The algorithm requires the right hand side

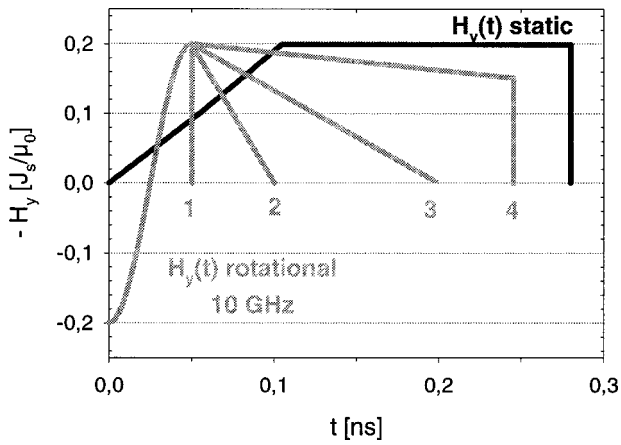


FIG. 1. Rotating magnetic field is applied in the (x,y) -plane and is switched off (#1) or slowly reduced (#2–#4) after a half cycle of rotation (0.05 ns).

of the LLG equation at specific times t_i . Whenever the right hand side of the LLG equation is evaluated Eq. (2) is used with $t=t_i$ to compute the current direction and strength of the external field.

In order to compare the different switching behavior, two different external field profiles $H(t)$ have been used for the simulations (Fig. 1). In the first case a homogeneous field was applied after rising the field from zero to $h = 0.2 J_s / \mu_0$ (160 kA/m for NiFe and 280 kA/m for Co) after $t=0.10$ ns. The unidirectional field was uniformly applied along the $-y$ direction of the system. Second, for comparison a half cycle (0.05 ns) of a rotating magnetic field with a frequency of 10 GHz was uniformly applied in the (x,y) -plane starting from field applied along the $+y$ direction. To show the influence of the resonance excitation, especially in NiFe, by abruptly turning off the rotating field, four different reduction speeds (#1 to #4) of the field strength to zero have been used for the simulations. To solve the Gilbert equation numerically the magnetic element is divided in finite elements. Table I summarizes the typical intrinsic material parameters used for the simulations.

The discretization of the Gilbert equation leads to an ordinary differential equation for every node for each com-

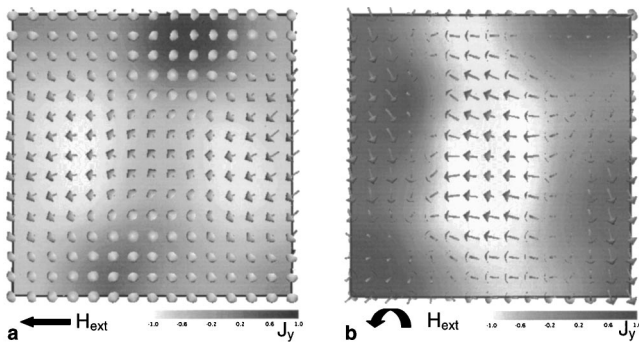


FIG. 2. Transient magnetization states within the $\text{Ni}_{80}\text{Fe}_{20}$ square during the reversal process for $H_{\text{ext}} = 160$ kA/m ($h = 0.2 J_s / \mu_0$) occurring in an unidirectional applied field along the y -direction at $t = 0.106$ ns leading to $\langle J \rangle = -0.49 J_s$ (a) and after the application of a 10 GHz rotational field in the (x,y) plane starting from the y -direction at $t = 0.073$ ns leading to $\langle J \rangle = -0.28 J_s$ (b).

TABLE I. Typical intrinsic material parameters used for the simulations, with J_s as saturation polarization, K_1 and K_2 as magneto-crystalline anisotropy constants and A as exchange constant.

Material	J_s [T]	K_1 [MJ/m ³]	K_2 [MJ/m ³]	A [pJ/m]
$\text{Ni}_{80}\text{Fe}_{20}$	1.00	0	0	13
Co-hcp ^a	1.76	0.45	0.15	13

^aAssuming uniaxial magneto-crystalline anisotropy parallel to the easy-axes of the grains.

ponent. The calculations were started from the remanent state after saturation parallel to the $+y$ -direction. The simulations were terminated at $J_y < 0.9 J_s$: Previous micromagnetic simulations have shown that the damping parameter α strongly influences the switching time.³ Shorter switching times are obtained at low external field strength values ($h < 0.5 J_s / \mu_0$). In the present study the Gilbert damping parameter was kept constant to $\alpha = 0.1$. Due to the small size, eddy currents are considered to be small and therefore are neglected.

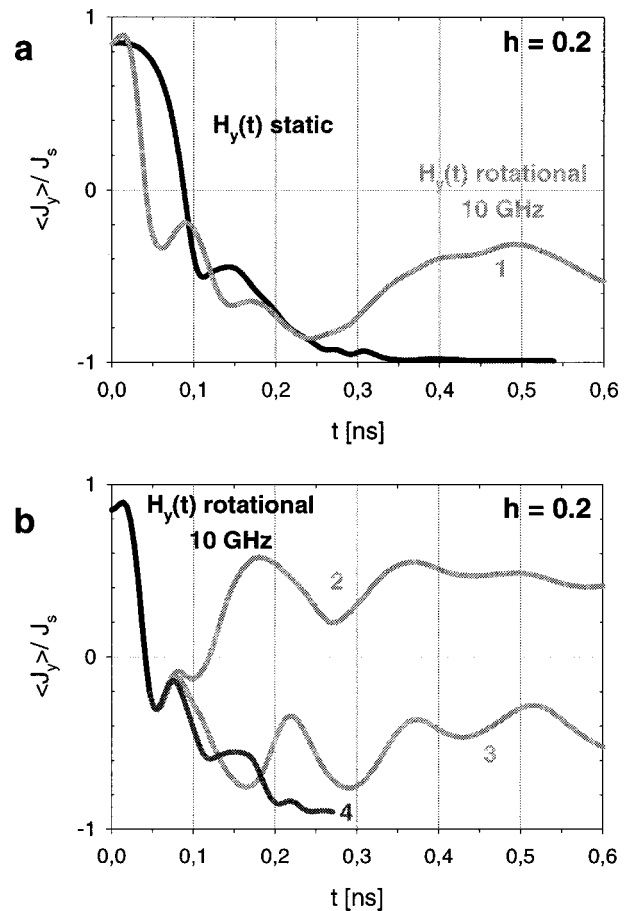


FIG. 3. Comparison of the time evolution of the polarization inside the $\text{Ni}_{80}\text{Fe}_{20}$ square element during the application of a unidirectional field after field rise and a half cycle of a rotating field at 10 GHz for $H_{\text{ext}} = 160$ kA/m ($h = 0.2 J_s / \mu_0$) for $\alpha = 0.1$ followed by abruptly switching off (a) and slow field reduction (b).

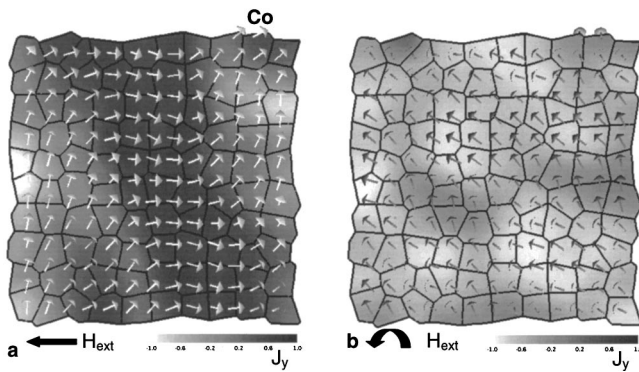


FIG. 4. Transient magnetization states within the polycrystalline Co square during the reversal process at $t=0.042$ ns occurring in an unidirectional applied field of $H_{\text{ext}}=100$ kA/m ($h=0.07 J_s/\mu_0$) leading to $\langle J \rangle=0.67 J_s$ (a) and during the application of a 10 GHz rotational field in the (x,y) plane starting from the y -direction of $H_{\text{ext}}=280$ kA/m ($h=0.2 J_s/\mu_0$) leading to $\langle J \rangle=-0.65 J_s$ (b).

III. RESULTS AND DISCUSSION

The numerical simulations show that in the case of the NiFe square with zero magnetocrystalline anisotropy the reversal process starts from the remanent state by rotating the magnetization in the end domains within the square during the rise time, if the field is applied uniformly along the $-y$ direction. The out of plane magnetization processes are clearly observed in the magnetization pattern of Fig. 2(a) which shows the transient magnetization state at $t=0.106$ ns. In contrary, the reversal process by the application of the rotational field of 160 kA/m reverses only 30% of the polarization after switching off the field. Figure 2(b) shows the magnetization pattern just after switching off the field ($t=0.073$ ns). The reversal starts in the center of the element, whereas the magnetization in the regions along the square edges only rotated by 90° . The diagrams of Fig. 3 compare the time evolution of the polarization component parallel to the applied field J_y , for the different field profiles $H(t)$, i.e., unidirectional field after a field rise from zero and rotational field, and maximum field strength values for the Ni₈₀Fe₂₀ thin film element. It obvious that the precessional oscillation effects of the polarization vector are strongly pronounced after abruptly switching off (#1) the high frequency rotational field at $t=0.05$ ns [Fig. 3(a)]. Despite the shorter switching time obtained by the rotational field the precessional instability hinders the square Ni₈₀Fe₂₀ element from a clear switching behavior. For the static field case and the rotational field at $h=0.2 J_s/\mu_0$ switching times ($\langle J_y \rangle=0$) less than 0.3 ns were calculated neglecting thermal activation processes. The numerical simulations show that in the NiFe square with zero magnetocrystalline anisotropy the reversal process starts from the remanent state by rotating the magnetization in the end domains within the square during the rise time, if the field is applied uniformly parallel to the $-y$ direction. The diagram of Fig. 3(b) shows the influence of the field reduction speed on the resonance excitations. Reducing the field slowly (#4) leads to a clear switching of the magnetization within $t=0.3$ ns.

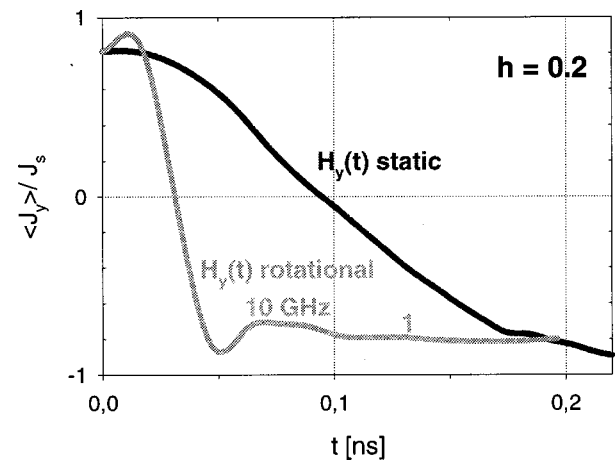


FIG. 5. Comparison of the time evolution of the polarization inside the polycrystalline Co square during the application of a unidirectional field and a rotating field at 10 GHz (rot) for $H_{\text{ext}}=160$ kA/m ($h=0.2 J_s/\mu_0$) for $\alpha=0.1$.

The granular thin Co film element is modeled with columnar grains generated from Voronoi polyhedrons. The transient magnetization states of Fig. 4(a) at $t=0.042$ ns indicate that nucleation and magnetization reversal partly occurs already during the rise time of the unidirectional applied field of 280 kA/m. Inhomogeneous magnetization rotation processes are dominant and lead the expansion of reversed domains starting from the edges perpendicular to the field direction. Under the influence of a constant, rotating field of 10 GHz the magnetization tries to follow the external field direction and starts to rotate in all grains leading to a nearly complete reversal of the polarization within a switching time of $t_{\text{sw}}=0.05$ ns [Fig. 4(b)]. Precessional oscillation effects, which occurred in the NiFe square, were obviously suppressed in the Co film assuming randomly oriented grains with uniaxial anisotropy (Fig. 5). We observed that the switching time decreases by a factor of about 10%, if the misorientation of the grains is assumed three dimensionally compared to a two dimensional texture within the film plane. The time evolution of the magnetization shows a clear switching in less than $t=0.05$ ns after abruptly switching off the high frequency rotating field (Fig. 5).

ACKNOWLEDGMENT

This work was supported by the Austrian Science Fund (P13260-TEC and Y-132 PHY).

- ¹R. Kikuchi, J. Appl. Phys. **27**, 1352 (1956).
- ²T. Leineweber and H. Kronmüller, J. Magn. Magn. Mater. **192**, 575 (1999).
- ³J. Fidler, T. Schrefl, V. D. Tsiantos, W. Scholz, and D. Suess, J. Comput. Phys. (in press).
- ⁴R. H. Koch, J. G. Deak, and D. W. Abraham, Phys. Rev. Lett. **81**, 4512 (1998).
- ⁵K. Zhang and D. R. Fredkin, J. Appl. Phys. **85**, 5208 (1999).
- ⁶W. Scholz, T. Schrefl, and J. Fidler, J. Magn. Magn. Mater. **233**, 296 (2001).
- ⁷J. Fidler and T. Schrefl, J. Phys. D **33**, R135 (2000).
- ⁸S. D. Cohen and A. C. Hindmarsh, Comput. Phys. **10**, 138 (1996).